Viscoelastic Indentation and Resistance to Motion of Conveyor Belts using a Generalized Maxwell Model of the Backing Material

Thomas J. Rudolphi [a] and Allen V. Reicks [b]

[a] Department of Aerospace Engineering, Iowa State University, Ames, IA
[b] Design Manager, Overland Conveyor, Inc., Denver, CO

Abstract

A one-dimensional Winkler foundation and a generalized viscoelastic Maxwell solid model of the belt backing material are used determine the resistance to motion of a conveyor belt over idlers. The viscoelastic material model is a generalization of the three-parameter Maxwell model that has previously been used to predict the effective frictional coefficient of the rolling motion. Frequency, or loading rate, and temperature dependence of the material properties are incorporated with the time/temperature correspondence principle of linear viscoelastic materials. As a consequence of the Winkler foundation model, a normalized indentation resistance is independent of the primary belt system parameters – carrying weight per unit width, idler diameter and backing thickness - as is the case for a three-parameter viscoelastic model. Example results are provided for a typical rubber compound backing material and belt system parameters.

Keywords: Rolling contact; Viscoelastic layer; Generalized Maxwell model; Winkler foundation; Indentation resistance

Introduction

Advances in rubber materials, belt fabrication and conveyor system technology, together with demands for larger systems to transport bulk granular materials, put a premium on efficient system design. The power to drive large conveyor systems is a critical design parameter, due to energy costs over the life of the system. Dissipative energy losses due to inelastic deformation and indentation of the belt covering, or "backing", material on a belt as it passes over each idler of the system is generally considered to be one of, if not the, dominant loss mechanism in the system. Hager and Hintz[1] estimate this source of power loss to be as much or greater than 60% of the total. Predictive analytical models of this loss are thus important to designers of such systems and several models have been developed and used.

The model of rolling resistance developed herein follows and builds on the work of several authors, including May, Morris and Atak[2], Jonkers[3], Spaans[4], Lodewijks[5,6] and Johnson[7]. These authors model the indentation of the idler into the backing as a one-dimensional stress/strain situation with the idler considered rigid and the backing as a Winkler foundation on a rigid base. Thus the compressed fibers, through the depth of the backing, act independently such that there is no accounting for shear in the deformation process. The full two-dimensional models of Hunter[8] and Morland[9] account for shear deformation, although they presume the backing to be a viscoelastic half-space, as opposed to having a finite depth, and require the solution of dual integral Equations to satisfy the contact equilibrium and deformation conditions.

More importantly, however, in the analyses mentioned above, the viscoelastic material behavior is presumed to be that of a simple, three-parameter Maxwell solid. However, rubber materials commonly used for backing on conveyor belts are highly temperature and load-rate dependent, so a useful viscoelastic constitutive model must accurately account for these effects. The three parameter model is extremely range limited, in both temperature and rate effects, to capture real viscoelastic behavior. In the present analysis, the three-parameter constitutive model is generalized to arbitrary $2N+1$ parameters, and used in combination with the Winkler foundation deformation model. Thermal and rate effects are incorporated through the well-accepted time/temperature superposition principle [9,10] of linear viscoelasticity to provide a simple, yet sufficiently comprehensive model of the deformation and material response, to capture realistic material behavior over a broad range of temperatures and load rates.

The Indentation Resistance Model

For a linear viscoelastic material and a one-dimensional state of stress, the stress relaxation formula for a prescribed strain history is determined by,[10]

$$\sigma(t) = \Psi(t)\varepsilon(0^+) + \int_0^t \Psi(t-s)\dot{\varepsilon}(s)ds \qquad (1)$$

where $\Psi(t)$ is the stress relaxation function, $\dot{\varepsilon} \equiv d\varepsilon/dt$ is the strain rate and $\sigma(t)$ is the stress at time t. For the present analysis the time $t = 0$ is taken to be that instant at which the belt first contacts the idler so that $\varepsilon(0^+) = 0$.
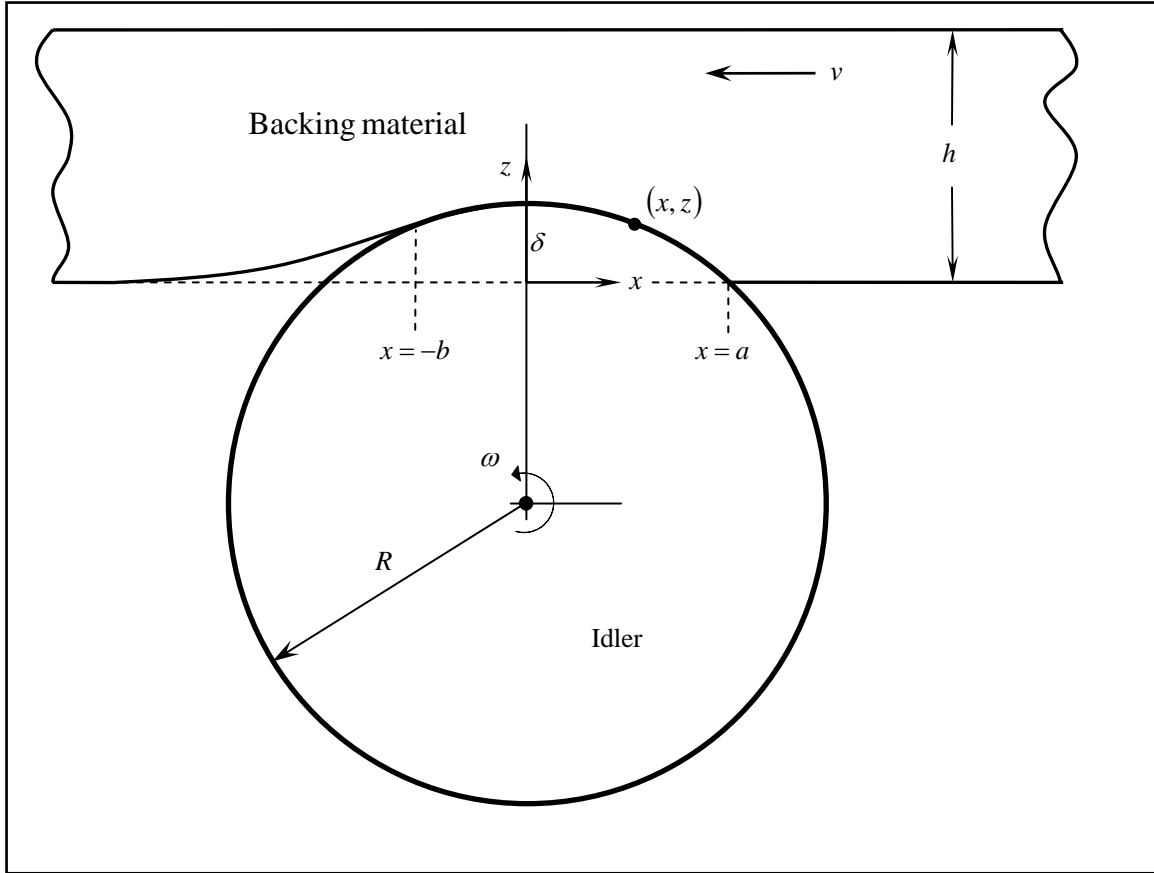
Figure 1. Indentation of the idler into the backing material and geometric parameters.

Following the work and general notational conventions of Jonkers[3], Spaans[4], Lodewijks[5,6] and Johnson[7], the kinematics of the deformation process for the belt backing passing over an idler at uniform speed v is shown in Figure 1. At a constant speed the deformation process is essentially steady state with respect to the Eulerian coordinate $x = a - vt$, where t denotes time and a the point of contact of the belt and idler (x is fixed with respect to the idler, but not rotating with it). The problem of steady motion may then be cast in terms of the coordinate x as opposed to the explicit time t through the above transformation.

For a small maximum indentation depth δ compared to the idler radius R, or $\delta/R \ll 1$, the indentation amount at a point x on the surface of the idler is approximated by a parabola such that $z = \delta - x^2/2R$, where $\delta = a^2/2R$. Hence the compressional strain of the backing material at the coordinate x, modeled as a Winkler foundation or independent linear elements through the backing, is

$$\varepsilon = \frac{z}{h} = \frac{1}{h}\left(\delta - x^2/2R\right) = \frac{1}{2Rh}\left(a^2 - x^2\right) \tag{2}$$

Using the translating coordinate speed relationship, $\dot{x} = -v$, so $\dot{z} = -2x\dot{x}/2R = xv/R$, the strain rate, or time derivative of Equation (2), becomes $\dot{\varepsilon} = \dot{z}/h = vx/Rh$. With this strain rate, the compressional stress between idler and belt, from Equation (1), may be expressed as a function of t or as a steady function of x,

$$\sigma = \int_0^t \Psi(t-s)\frac{v}{Rh}(a-vs)ds = -\frac{1}{Rh}\int_a^x \Psi\left(\frac{\xi-x}{v}\right)\xi\,d\xi \qquad (3)$$

Now, for a given material relaxation function Ψ, this Equation can, in principle, be integrated to explicitly determine the contact stress profile between the belt and the idler as depicted in Figure 2. However, the contact length $a+b$, or both the point of first contact a and the point of departure b, are undetermined; they depend on the load or net
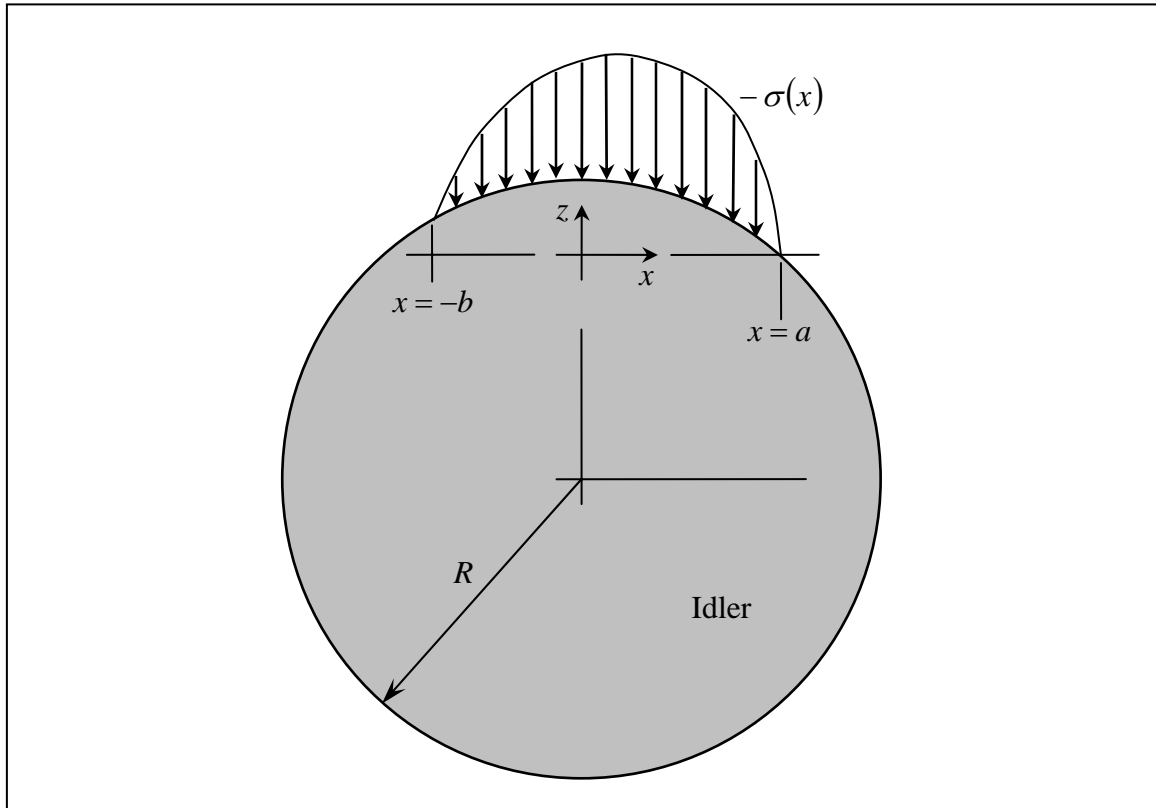

Figure 2. Contact stress distribution between idler and backing.

force between the belt and idler, and hence, as in most situations involving contacting materials, this problem is geometrically nonlinear.

At equilibrium, the load W (force per unit width across the idler) and the resultant of the stress distribution must be in balance such that

$$W = \int_{-b}^a \sigma(x)dx \qquad (4)$$

To determine a and b, Equations (3) and (4) must be satisfied simultaneously, but an explicit solution is not possible. However, as shown by Lodewijks[5], a simple iterative procedure can be used to balance the load and the contact length, determining both a and b, given the load W.

Once the stress profile and contact length is determined, the moment M of the stress distribution about the center of the idler is

$$M = \int_{-b}^{a} x\sigma(x)dx \qquad (5)$$

Then the resistance force to rolling is M/R and the coefficient of rolling resistance, or equivalent Coulomb drag coefficient μ, is

$$\mu = \frac{M}{RW} = \frac{1}{R}\frac{\int_{-b}^{a} x\sigma(x)dx}{\int_{-b}^{a} \sigma(x)dx} \qquad (6)$$

In the following section, the above Equations are evaluated, incorporating the generalized material model, to provide a closed form model for the indentation resistance.

The Generalized Maxwell Material Model

For rubber compounds used as backing for belt conveyors, it is common to use the simple three-parameter Maxwell constitutive model. For realistic backing materials, however, the three parameter model is not capable of representing viscoelastic behavior over a range of temperatures and loading rates. The three parameter model is easily generalized to $2N+1$ parameters as shown in Figure 3, or to what is sometimes called the Zenar
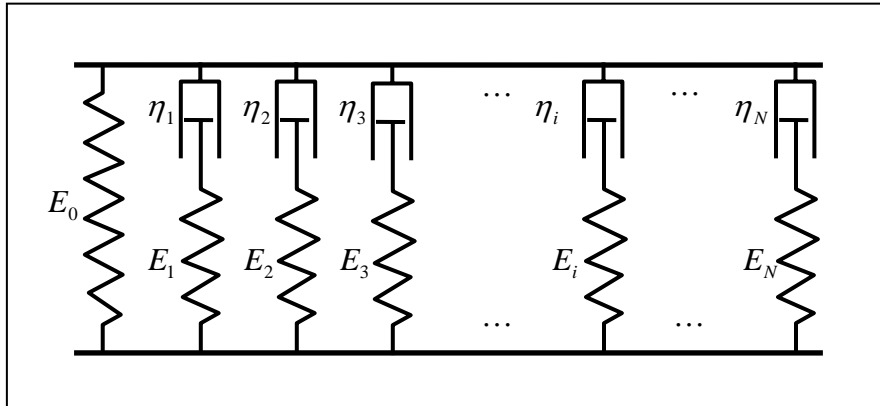

Figure 3. The mechanical elements of the Maxwell solid model.

model. The constants E_i and η_i represent the various elastic and dissipative viscous elements of the model and the constant E_0 is referred to as the long term or equilibrium modulus.

According to this generalized $2N+1$ parameter model, the stress response function is given by the Prony series[11]

$$\Psi(t) = E_0 + \sum_{i=1}^{N} E_i e^{-t/\tau_i} \qquad (7)$$

where $\tau_i = \eta_i / E_i$ are the characteristic periods of the various dissipative elements of the mechanical model. Insertion of this response function into Equation (3) for the stress, including the transformation $t = (a-x)/v$, one has,

$$Rh\sigma(t) = -\int_a^x \left[E_0 + \sum_{i=1}^N E_i e^{-(\xi-x)/v\tau_i} \right] \xi \, d\xi \tag{8}$$

Then, similar to the 3-parameter model, each term of series in this Equation can be integrated to arrive at the result,

$$\frac{Rh}{a^2}\sigma(x) = \frac{E_0}{2}\left(1-\frac{x}{a}\right)\left(1+\frac{x}{a}\right) + \sum_{i=1}^N E_i k_i \left[(1+k_i)\left(1 - e^{-\frac{1}{k_i}\left(1-\frac{x}{a}\right)}\right) - \left(1-\frac{x}{a}\right) \right] \tag{9}$$

where $k_i = v\tau_i / a$ are the Deborah (wave) numbers corresponding to the N element pairs of the material model.

Now, introducing the non-dimensional length parameter $\varsigma = b/a$, and equating the stress of Equation (8) to zero at $x = -b$ provides the condition,

$$\frac{E_0}{2}(1+\varsigma)(1-\varsigma) + \sum_{i=1}^N E_i k_i \left[k_i - \varsigma - (1+k_i)e^{-(1+\varsigma)/k_i} \right] = 0 \tag{10}$$

For given material parameters, the solution of this Equation would provide only the ratio $\varsigma = b/a$, not a or b explicitly. The additional condition that must be satisfied is Equation (4), which, when integrated and also expressed in terms of ς is

$$\frac{Rh}{a^3}W = \frac{E_0}{6}\left(2+3\varsigma-\varsigma^3\right) + \sum_{i=1}^N E_i k_i \left\{ \frac{1}{2}\left(1-\varsigma^2\right) - k_i\left[(1+k_i)\left(1-e^{-(1+\varsigma)/k_i}\right) - (1+\varsigma)\right] \right\} \tag{11}$$

Then, for given material parameters E_i, k_i, and belt system parameters W, R and h, the values of ς and a, which satisfy both Equations (10) and (11), will be in equilibrium with the load W. The simultaneously solution is readily accomplished numerically by a simple iterative procedure:

(a) Initialize a guess for ς and solve Equation (11) for a.

(b) Use this value of a to determine the material parameters $k_i = v\tau_i / a$.

(c) With these values of k_i and E_i, solve (numerically) Equation (10) for ς.

(d) Use the updated value of ς, replace the initial guess of step (a) and continue repetition of steps (a), (b) and (c) until ς converges to a predetermined accuracy.

Following this iterative process to determine an accurate value of $\varsigma = b/a$, a and b, Equation (5) can then be evaluated to get the moment of the stress distribution. Thus,

$$M = \frac{E_0 a^4}{8R^2 h}\left(1-2\varsigma^2+\varsigma^4\right) + $$
$$\sum_{i=1}^N \frac{E_i a^4 k_i}{R^2 h}\left[k_i^3 - \frac{k_i}{2}\left(1+\varsigma^2\right) + \frac{1}{3}\left(1+\varsigma^3\right) - k_i(1+k_i)(k_i+\varsigma)e^{-(1+\varsigma)/k_i} \right] \tag{12}$$

The indentation resistance coefficient then follows from Equations (6), (11) and (12).

Combining these Equations in such a way as to eliminate the explicit appearance of the contact length parameter a, Equation (6) can be written as

$$\mu = \frac{1}{R}\left(\frac{M}{W}\right) = \left(\frac{Wh}{E_0 R^2}\right)^{1/3} \frac{M^*}{\left(F^*\right)^{4/3}} \tag{13}$$

where the non-dimensional functions F^* and M^* have been introduced and are given by,

$$F^*(\varsigma) \equiv \frac{1}{6}\left(2 + 3\varsigma - \varsigma^3\right) + \sum_{i=1}^{N}\left(\frac{E_i}{E_0}\right)k_i\left\{\frac{1-\varsigma^2}{2} - k_i\left[(1+k_i)\left(1 - e^{-(1+\varsigma)/k_i}\right) - (1+\varsigma)\right]\right\} \quad (14)$$

$$M^*(\varsigma) \equiv \frac{1}{8}\left(1 - 2\varsigma^2 + \varsigma^4\right)$$

$$+ \sum_{i=1}^{N}\left(\frac{E_i}{E_0}\right)k_i\left[k_i^3 - \frac{k_i}{2}\left(1+\varsigma^2\right) + \frac{1}{3}\left(1+\varsigma^3\right) - k_i(1+k_i)(k_i + \varsigma)e^{-(1+\varsigma)/k_i}\right] \quad (15)$$

In both these functions, the moduli have been normalized to E_0, giving rise to the ratio $\left(E_i/E_0\right)$ in each expression and introduces the non-dimensional factor $\left(Wh/E_0R^2\right)^{1/3}$ as a coefficient of μ in Equation (13).

Equation (12) then shows the direct dependence of μ on $\left(Wh/R^2\right)^{1/3}$, as is a direct consequence of the Winkler foundation model and consistent with the results of the three parameter material models of other[3-6]. Inclusion of E_0 in this factor renders it non-dimensional. Reflecting this factor, a normalized indentation factor F is defined by,

$$F \equiv \mu\left(\frac{Wh}{E_0R^2}\right)^{-1/3} = \frac{M^*}{\left(F^*\right)^{4/3}} \quad (15)$$

It is noted that since this normalized indentation factor is the ratio of two terms that depend only on the material parameters k_i and E_i, so after the load dependent factor ς has been determined by the iterative process described above, then F is solely a function of the backing material viscoelastic properties. As such, F is independent of the belt system parameters W, h and R, unlike the coefficient μ, is essentially a material property from which the indentation resistance can be determined for any W, h and R.

Temperature Dependent Material Modeling

Mechanical properties of a viscoelastic material are typically measured by cyclically-imposed deformation tests on standard specimens in simple extension, shear, bending or torsion at controlled temperatures and at relatively low frequencies to avoid inertial effects. By testing over a wide temperature range but limited frequencies, and using the superposition principle, which relates time (equivalently frequency or speed) and temperature effects, one can extrapolate to frequencies or load rates considerably beyond those of the test. This theoretical rheological model for viscoelastic materials, supported by experimental measurements, and postulating the equivalence of temperature and time effects, is known as the time/temperature superposition principle[9,10]. According to this principle, if T denotes temperature and T_0 a reference temperature, then a material property at time t and temperature T is equivalent to that at time $a_T t$ and temperature T_0, where a_T is a "shift" parameter in time so that $a_T = a_T(T,T_0)$. A commonly used expression for a_T, applicable to amorphous polymers at temperatures above the glass transition temperature T_g, due to Williams, Landel and Ferry[12] and referred to as the WLF Equation, is the logarithmic form, $\log(a_T) = C_1(T - T_0)/[C_2 + (T - T_0)]$, where C_1 and C_2 are constants determined empirically from data.

Alternately, for data taken from cyclical or frequency controlled strain experiments, an empirical representation of the time/temperature shift parameter a_T may be determined by overlaying, through shifts in the frequency, the temperature dependent modulus data onto a "master" curve. The required frequency shift, on a logarithmic scale, for data at each test temperature, to produce the overlay determines the equivalent of the WLF Equation, or may be taken the basic temperature/frequency relationship of the superposition principle. This master curve approach is used here to relate temperature and frequency, or load rate effects, within the generalized Maxwell material model. So instead of the above functional form for a_T of the WLF Equation with only two constants, the relationship between a_T and temperature T is taken as,

$$\log(a_T) = \sum_{i=0}^{n} a_i T^i = a_0 + a_1 T + a_2 T^2 + \cdots + a_n T^n \qquad (16)$$

and the constants a_i are determined by a least squares curve fitting process in the construction of the master curve for the material.

Experimental measurement of the mechanical properties of polymeric materials is most often done by subjecting specimens to cyclic strain programs at fixed temperatures and over a limited range of frequencies. For a sinusoidal strain history of the form $\varepsilon = \varepsilon_0 \sin(\omega t)$, where ω is the circular frequency and ε_0 the amplitude, and after an initial transitory state, the stress follows the strain in frequency, but at a delayed phase. For elastic material, the stress and strain are in phase, but for viscoelastic materials there is a delayed response, and it is convenient to express this relationship in the form[10],

$$\sigma(t) = E^*(\omega)\varepsilon(t) = \left[E'(\omega)^2 + E''(\omega)^2\right]^{1/2} \varepsilon_0 \sin(\omega t + \delta) \qquad (17)$$

where E^* is the magnitude of the complex modulus with real and imaginary components $E'(\omega)$ and $E''(\omega)$, called the storage and loss moduli, respectively, and $\delta(\omega) = E''(\omega)/E'(\omega)$ is the phase angle or lag of stress behind strain. For the generalized Maxwell model, the storage and loss moduli are related to the mechanical elements of the model shown in Figure 3 by [11],

$$E'(\omega) = E_0 + \sum_{i=1}^{N} E_i \frac{\omega^2 \tau_i^2}{1 + \omega^2 \tau_i^2} \qquad (18)$$

and

$$E''(\omega) = \sum_{i=1}^{N} E_i \frac{\omega \tau_i}{1 + \omega^2 \tau_i^2} \qquad (19)$$

where E_i are now the discrete or spectral values of the Maxwell model and $\tau_i = \eta_i / E_i$ are the periods of the various elements.

Implicit in material properties $E'(\omega)$ and $E''(\omega)$ is the dependence on temperature. In the frequency domain, the superposition principle relates properties at temperatures and frequencies according to the relationships

$$E'(\omega, T) = E'(a_T \omega, T_0), \quad E''(\omega, T) = E''(a_T \omega, T_0) \qquad (20)$$

From these Equations, which represent the material's master curves of $E'(\omega)$ and $E''(\omega)$, one can extrapolated to frequencies, and hence loading rates, considerably

beyond those of the test data. For a given belt speed v, the relationship between load rate and frequency is taken to be

$$\omega = \frac{\pi v}{a+b} \tag{21}$$

which derives from the presumption that an element of the material of the backing passes through a half-cycle of loading during the contact period. This Equation, which couples the material properties and contact length, and hence the material properties to the deformation and equilibrium Equations, through the iterative process outlined previously for Equations (10) and (11) in the establishment of a and b.

Figures 4 and 5 show the combination master curves and shift factor of the shear moduli $G'(\omega) = E'(\omega)/3$ and $G''(\omega) = E''(\omega)/3$ for a typical, incompressible, belt backing material. These curves were constructed from data taken in a twisting/shear mode test over a temperature range of -60° to $+70^{\circ}C$ at about 10° increments and frequencies from 0.01 to $15\,Hz$ with about 13 equally spaced increments on a logarithmic scale. The shift factor a_T of Figure 5 was developed according to Equation (16), from the data at each temperature increment, starting from a chosen reference temperature.
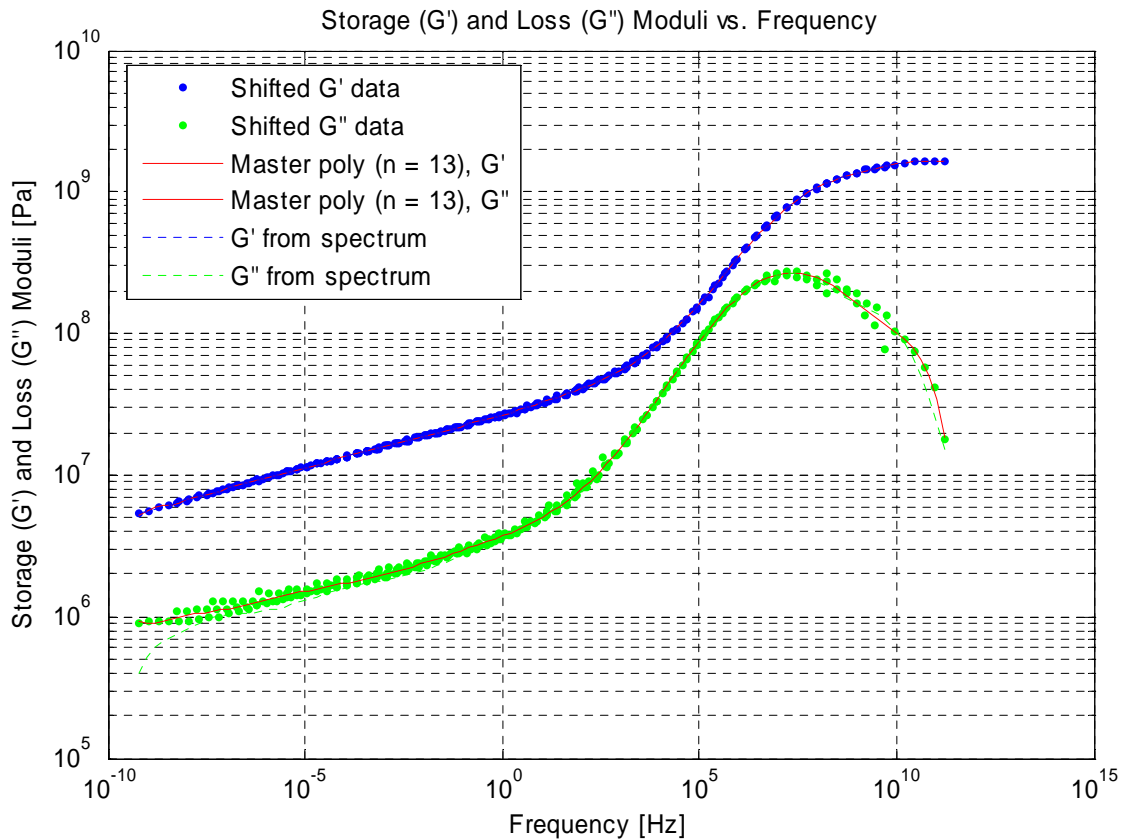

Figure 4. Master curve for a typical belt backing material.

The reference temperature for this curve is $0^{\circ}C$, which is where a_T equals 1 of Figure 5, and a polynomial of order 5 is shown on the curve with the discrete a_T values of the fitting process, as prescribed by Equation (16).
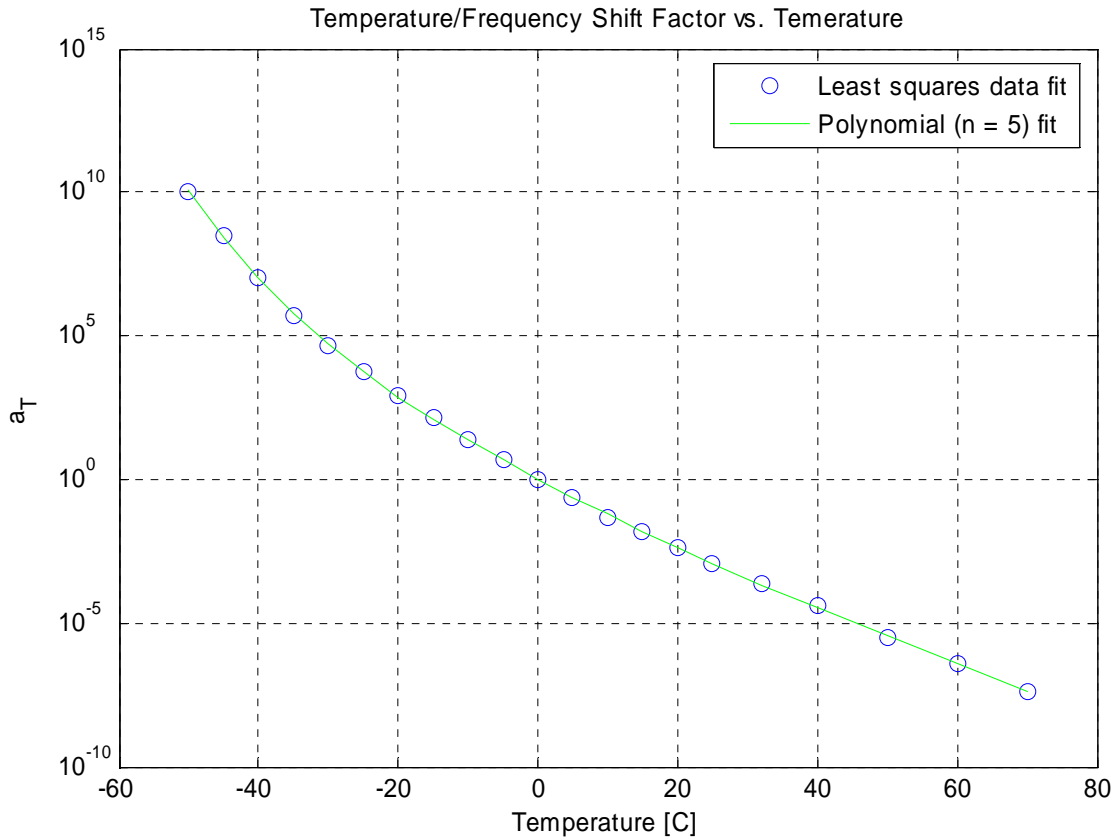
Figure 5: Frequency/temperature shift factor.

For this material, as characterized by the master curve and frequency/temperature shift factor, the discrete $2N+1$ parameters of the Maxwell model, i.e., values of E_i and η_i of Equations (17) and (18) are also determined. This amounts, equivalently, to the determination of the discrete spectrum of the material, where Equations (18) and (19) represent the discrete versions of comparable continuous transforms.

Determination of these discrete spectral values has been the focus of much research and various techniques and mathematical fitting processes – Tschoegl[13] and Emri and Tschoegl[14]. Neural networks and genetic algorithms have also been employed to "best fit" both E_i and η_i, or equivalently E_i and τ_i, from given data as in Figure 4. Alternately, a common and fairly simple approach is to fix the periods $\tau_i = 1/\omega_i$ at values equally spaced on the $\log(\omega)$ scale (half-decade increments is sufficient[13]) and then use a least square curve fit to the "data" as calculated from the polynomial fit of the master curve at the $\tau_i = 1/\omega_i$ values over the range of the data. Here, a non-linear, non-negative, least square method is used to fit the data. The non-negative constraint on the fitting process is not necessary, but eliminates the possibility of negative E_i coefficients, which is not uncommon for this type of transform[13].

Figure 6 shows the resulting spectral values that result from fitting the G' master curve to Equation (18). The re-calculate values of G' and G'' that result from the

spectrum, through Equations (16) and (17) are shown in the original master curves in Figure 4. Note that the re-calculated G' is accurate, since the spectrum is fit to this "data", but also the calculation of G'' from the spectrum derived from fitting G' is also
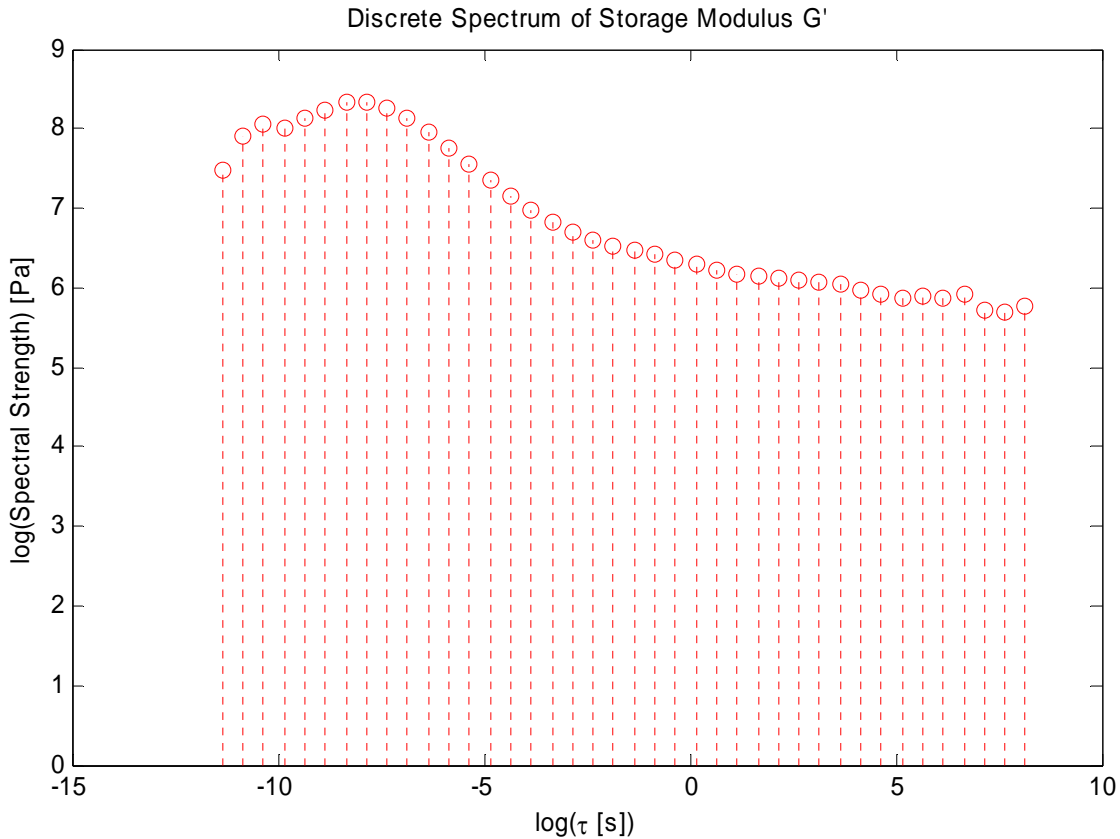

Figure 6.   *Discrete spectrum of the storage modulus G'.*

accurate over the range of the data. Some deviation is evident at the frequency extremes, but the consistency of the fit is evidence of the redundancy involved in the spectral characterization of both Equations (16) and (17).

Indentation Resistance Calculations

With the discrete spectrum of Figure 6 as a characterization of a typical backing material, the indentation resistance model of Equations (10) – (15) were evaluated for a range of temperatures and belt speeds, and at typical values of system parameters: $W = 10\,lb/in = 1751.3\,N/m,\quad h = 0.25\,in = 0.00635\,m\quad R = 3\,in = 0.0762\,m$. Belt speed, being a function of time, relates also to temperature through the superposition principle, which allows for the construction of universal curves of μ and F, for any temperature/speed combination when graphed as functions of va_T. Thus, Figures 7 and 8 give, respectively, the friction coefficient μ of Equation (13) and the non-dimensional value F of Equation
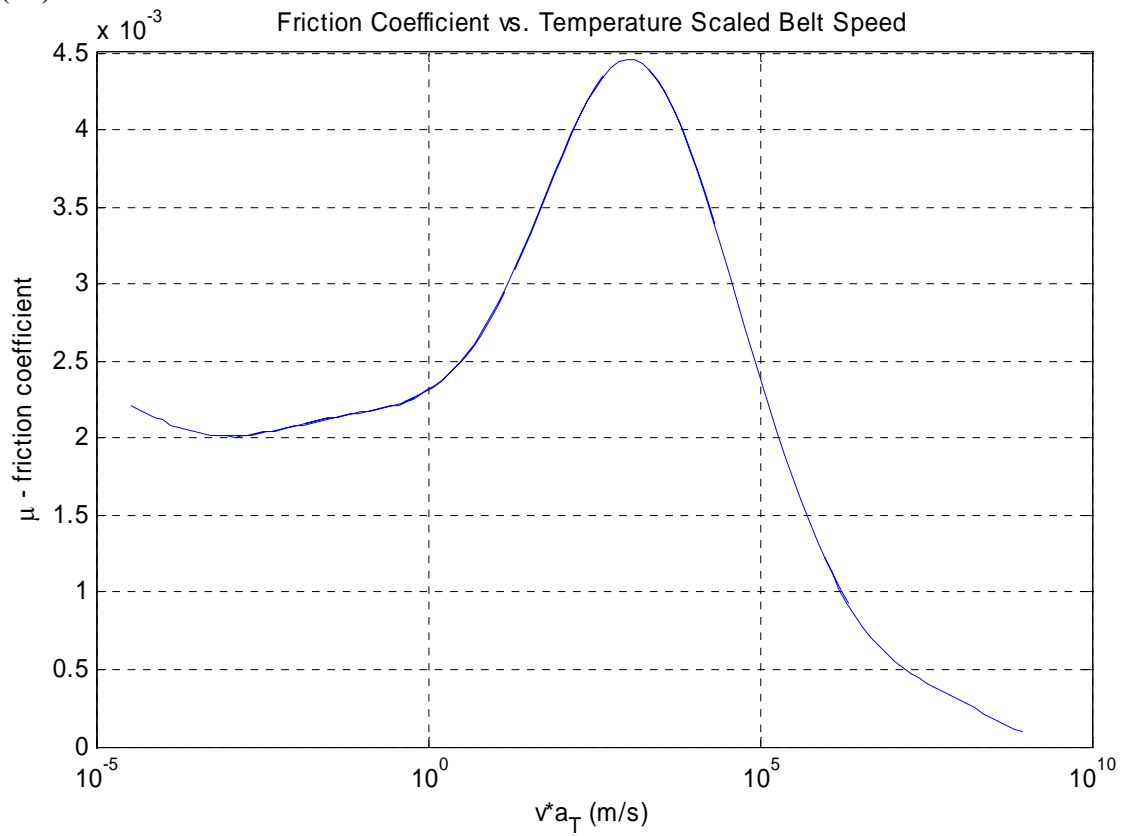
(13).

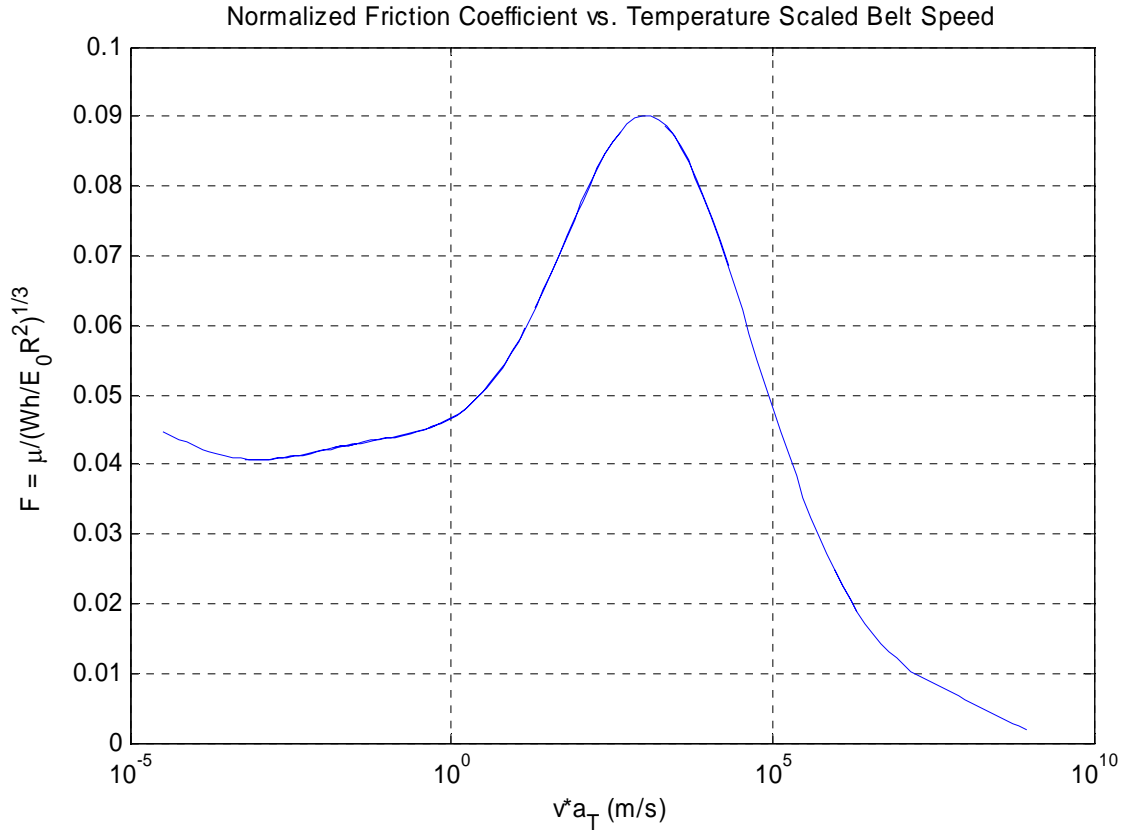*Figure 7: Indentation resistance μ vs. scaled belt speed.*

Figure 8. Normalized indentation resistance F vs. scaled belt speed.

These graphs are actually composites, or overlapping segments, of the calculation of μ and F through the algorithm above, with the calculations performed through nested loops through increments in the temperature T and speed v. When graphed against va_T, these resulting curves actually overlap, but the overlapping portions are only faintly visible in the graphs, which is a consequence of the superposition principle. Thus, Figures 7 and 8 are universal curves, implicit in temperature, i.e., applicable to all temperatures in the range provided by the shift parameter a_T of Figure 5.

Determination of specific values of μ or F from the curves of Figures 7 and 8, at given values of the belt speed v and temperature T, is then done in conjunction with the a_T curve of Figure 5. Given T, one would first find the value of a_T from Figure 5, providing the ordinate va_T for the corresponding value of μ and F from Figures 7 and 8. Thus, for this material at a temperature of, say, $T = -20^{\circ}C$, Figure 5 provides a value $a_T \approx 10^3$, and at a speed of $2\,\mathrm{m/s}$ so that $va_T = 2 \times 10^3$ m/s, the values of μ and F from Figures 7 and 8 would be located on the curves just at about the peaks of the curves and be about 0.0044 and 0.089, respectively. As noted previously, utility of the non-dimensional F of Figure 8 is that it pertains to systems with any values of W, h and R.

For the same material and calculations, Figure 9 shows the corresponding contact length parameter $\varsigma = b/a$ as results from the iteration process at which the load W is in equilibrium with the contact stress. It is noted here that a minimal value of ς occurs at

$va_T \approx 10^3$ m/s, which, not surprisingly, is the same speed/temperature at which the indentation resistance factors μ and F attain their maximum values.
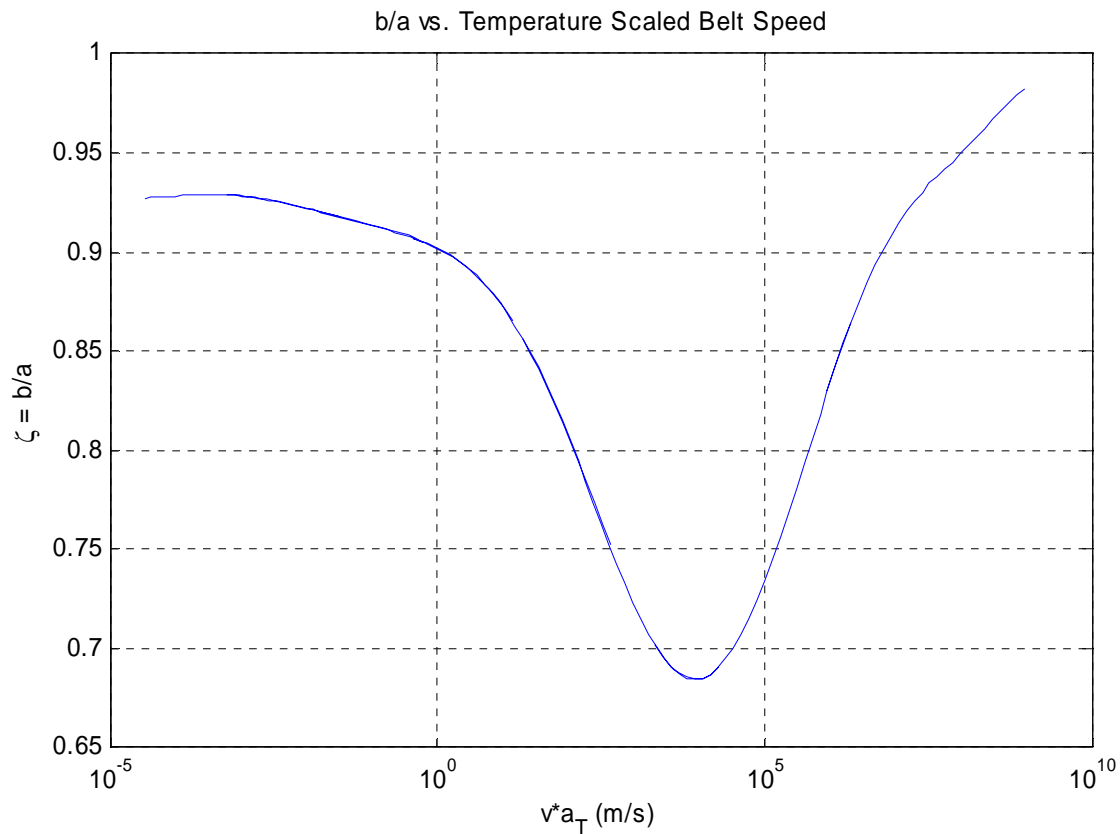

Figure 9. Contact length ratio vs. scaled frequency.

Discussion and Conclusions

A predictive model of the indentation and rolling resistance of a linear viscoelastic material backing on a conveyor belt using a generalized Maxwell material model of the backing material has been made. This represents a generalization of the three parameter model that has traditionally been used for the calculation of the indentation resistance, but which is capable of capturing the real polymeric behavior of rubber backings used on large, modern conveyor systems. The viscoelastic layer is presumed to be one dimensional in the sense of that of a Winkler foundation.
 Explicit formulae for the resistance coefficient were developed and sample calculations with material properties typical of a common backing material were made. The particular material considered in the example calculations shows the typical peaking of the indentation resistance at some point in the temperature/speed range. As an aid to design and minimization of the power required for conveyor systems, the developed methodology is directly usable for the evaluation of the performance of the backing material, once the material properties are established through standard testing methods.

References

[1] M. Hager and A. Hintz, The energy-saving design of belts for long conveyor systems, Bulk Solids Handling, 13, 4 (1993), pp. 749-758.

[2] W.D. May, E.L. Morris and D. Atack, Rolling friction of a hard cylinder over a viscoelastic material, Journal of Applied Physics, 30, 11 (1959), pp. 1713-1724.

[3] C.O. Jonkers, The indentation rolling resistance of belt conveyors: A theoretical approach, Fördern und Heben, 30, 4 (1980), pp. 312-317.

[4] C. Spaans, The calculation of the main resistance of belt conveyors, Bulk Solids Handling, 11, 4 (1991), pp. 1-16.

[5] G. Lodewijks, The rolling resistance of conveyor belts, Bulk Solids Handling, 15, 1 (1995) 15-22.

[6] G. Lodewijks, Design of high speed belt conveyors, Bulk Solids Handling, 19, 4 (1999), pp. 463-470.

[7] K.L. Johnson, Contact Mechanics, Cambridge University Press, Cambridge, UK, 1985.

[8] S.C. Hunter, The rolling contact of a rigid cylinder with a viscoelastic half space, Journal of Applied Mechanics, 28 (1961), pp. 611-617.

[9] L.W. Morland, A plane problem of rolling contact in linear viscoelasticity theory, Journal of Applied Mechanics, 29 (1962), pp. 345-352.

[10] A.S. Weinman and K.R. Rajagopal, Mechanical Response of Polymers: An Introduction, Cambridge University Press, Cambridge, UK, 2000.

[11] J.D. Ferry, Viscoelastic Properties of Polymers, 3rd Edition, Wiley, New York, 1980.

[12] M. Williams, R. Landel and J. Ferry, The temperature dependence of relaxation mechanisms in amorphous polymers and other glass-forming liquids, Journal of the American Chemical Society, 77 (1955), p. 3701.

[13] N. W. Tschoegl, The Phenomenological Theory of Linear Viscoelastic Behavior: An Introduction, Springer, Berlin, 1989.

[14] I. Emri and N.W. Tschoegl, Generating line spectra from experimental responses. Part I: Relaxation modulus and creep compliance, Rheologica Acta, 32 (1993), pp. 311-321.